Artificial
Organs

Artificial Organs
34(2):E34–E45, Wiley Periodicals, Inc.

Noninvasive Activity-based Control of an Implantable Rotary Blood Pump: Comparative Software Simulation Study

*†Dean M. Karantonis, *Einly Lim, ‡David G. Mason, §Robert F. Salamonsen, ¶Peter J. Ayre, and *Nigel H. Lovell

**Graduate School of Biomedical Engineering, University of New South Wales; †School of Electrical Engineering and Telecommunications, University of New South Wales, Sydney, New South Wales; ‡Department of Surgery, Monash University; §Cardiothoracic Intensive Care, The Alfred Hospital, Melbourne, Victoria; and ¶Ventracor Limited, Sydney, New South Wales, Australia*

Abstract: A control algorithm for an implantable centrifugal rotary blood pump (RBP) based on a noninvasive indicator of the implant recipient's activity level has been proposed and evaluated in a software simulation environment. An activity level index (ALI)—derived from a noninvasive estimate of heart rate and the output of a triaxial accelerometer—forms the noninvasive indicator of metabolic energy expenditure. Pump speed is then varied linearly according to the ALI within a defined range. This ALI-based control module operates within a hierarchical multiobjective framework, which imposes several constraints on the operating region, such as minimum flow and minimum speed amplitude thresholds. Three class IV heart failure (HF) cases of varying severity were simulated under rest and exercise conditions, and a comparison with other popular RBP control strategies was performed. Pump flow increases of 2.54, 1.94, and 1.15 L/min were achieved for the three HF cases, from rest to exercise. Compared with constant speed control, this represents a relative flow change of 30.3, 19.8, and –15.4%, respectively. Simulations of the proposed control algorithm exhibited the effective intervention of each constraint, resulting in an improved flow response and the maintenance of a safe operating condition, compared with other control modes. **Key Words:** Implantable rotary blood pump—Pumping states—Control strategy—Left ventricular assist device.

Congestive heart failure (HF) is a serious health condition which affects an estimated 300 000 Australians (over 45 years of age) (1), 2.4 million Americans (2), and 676 500 UK citizens (3). Furthermore, HF in the USA causes 39 000 deaths a year and is a contributing factor in another 225 000 deaths (2). While the drug-based palliation of such a highly prevalent condition is an advancing field, improving the quality of life for those individuals suffering with end-stage HF has been a difficult task. Transplantation of the heart, which is available to a small minority of HF sufferers due to the lack of donor organs, is the only definitive therapy for those with severe cases of HF. The increasing availability of mechanical left ventricular assist devices (LVADs), however, offers new opportunities for the treatment of these individuals. In particular, third-generation implantable rotary blood pumps (RBPs) serving as LVADs are hoped to provide not only a bridge-to-transplant option, but also a destination therapy (i.e., lifetime) solution, via their portability and inherently superior long-term reliability compared to previous LVAD technologies. As such, the prospects for HF sufferers shall improve in the coming years as these devices become a mature technology.

One of the critical goals necessary for improving the state of RBP technology involves the development of a control strategy, which automatically adjusts the pump speed to cater for changes in metabolic demand. In a healthy individual, the pumping action of the heart is governed by the Frank–Starling

doi:10.1111/j.1525-1594.2009.00932.x

Received April 2009; revised July 2009.
Address correspondence and reprint requests to Professor Nigel H. Lovell, Graduate School of Biomedical Engineering, University of New South Wales, Sydney, NSW 2052, Australia. E-mail: N.lovell@unsw.edu.au

mechanism. This mechanism ensures that left ventricle (LV) stroke volume is adjusted to compensate for changes in LV end-diastolic volume or its correlate preload (which refers to the end-diastolic sarcomere length of cardiac muscle fibers), such that the LV ejects whatever volume of blood it receives. Pulsatile LVADs, which sense the volume of their artificial ventricle, operate according to this principle. In contrast, RBPs are relatively insensitive to preload (4), meaning they cannot inherently determine or sense the amount of blood with which they are supplied. Therefore, it is imperative that a pump control strategy maintains a safe operating range where pump outflow matches right heart output. Failure to do so may lead to either ventricular collapse due to over-pumping or a fall in preload, or reverse pump flow (regurgitation) and pulmonary edema as a result of under-pumping and associated fall in applied pump differential pressure (5–7). These undesirable conditions are potentially harmful to the patient, and must be readily detectable and avoided in implant recipients. Furthermore, the ability to estimate the instantaneous values of pump flow (Q_p) and differential pressure (ΔP) (often referred to as pump head [H]) is of utmost importance for a pump control strategy (8,9). For instance, ensuring a minimum mean pump flow rate is achieved or a maximum differential pressure constraint is met will require an accurate estimate of these variables to be made.

Present clinical practice involves the setting of a constant mean pump speed for each patient based on their current condition. This approach requires regular supervision by clinicians, to ensure the set speed continues to provide a safe operating state for the patient. However, in order to regain a normal lifestyle, it is highly desirable for the patient to be discharged from the hospital. In such a long-term unsupervised environment, an automated control strategy is needed to replace the clinician, whereby the RBP adapts to the patient's current physiological state.

Each of the algorithms defining the control modules mentioned above—including Q_p and ΔP estimation, and ventricular suction detection—have been developed and discussed previously by the authors (6,8,10–13). The present study introduces a pump control strategy with multiple objectives, combining each of these modules with a control mechanism, which aims to adjust pump speed according to an estimate of the patient's level of physical activity. Importantly, the approach is based entirely on noninvasive pump feedback signals. Thus, the issues of reduced reliability and relatively higher cost associated with incorporating implanted sensors are avoided. Using a software model of the human cardiovascular system (CVS) and centrifugal RBP under evaluation (Ventrassist LVAD, Ventracor Limited, Chatswood, Australia), the new control strategy was evaluated and compared with three existing popular strategies: pulsatility control (4,14–17), pump differential pressure control (18–23), and constant target speed control. The ability of these control modes to satisfy the physiological requirements of each simulated implant recipient was the key determinant of their performance.

METHODS

Physiological requirements

Maintaining circulatory homeostasis in HF requires optimization of many physiological variables, including cardiac output (CO), right and left ventricular systolic pressures, left and right atrial pressures, heart rate (HR) and rhythm, and blood volume. Implantation of an LVAD, depending on its means of control, can make this more taxing. One specification for optimum balance, as described by Boston et al. (24) suggests:

- CO must be sufficient for the metabolic requirements of the body both at rest and in exercise.
- Systolic arterial pressure should be maintained between patient specific limits. Excessive levels can lead to a number of conditions (such as atherosclerosis, stroke, or kidney failure) while inadequate pressures impair the autoregulation of tissue blood flow.
- Left atrial pressure (LAP) should be controlled to less than 15 mm Hg to avoid pulmonary edema and above 0 mm Hg to avoid ventricular suction.

A new control parameter: the activity level index (ALI)

In order to meet the objective of developing a demand-responsive control strategy, a novel control parameter referred to as the ALI was conceived. ALI is based on two other parameters that are measured noninvasively:

1 Triaxial accelerometer (TA)

A TA measures the acceleration components of a moving object in three orthogonal axes. Numerous research groups (25–29) have examined the ability of TA devices to estimate energy expenditure and various other parameters associated with gait and posture. In particular, the signal magnitude area (SMA) of the TA output has been reported to be highly correlated (on a per-user basis) with metabolic

energy expenditure (26,28,30) when the device is mounted on the wearer's torso (hip or back). The SMA is the sum of the absolute integrals of the three orthogonal acceleration vectors, measured in units of *g* (acceleration due to gravity), and represented mathematically as in Eq. 1. It should be noted that the acceleration vector inputs are high-pass filtered to remove the gravitational component of the signal.

$$SMA = \int_{t_0}^{t_0+T} |x|\,dt + \int_{t_0}^{t_0+T} |y|\,dt + \int_{t_0}^{t_0+T} |z|\,dt \qquad (1)$$

2 HR estimate

HR is a valuable indicator of the exercise state of an individual (31–34), and an estimate of its value in LVAD recipients may be obtained via analysis of the pump speed waveform. Each time the native heart contracts, the increased pump flow escalates the amount of force or torque on the impeller, temporarily causing impeller speed to fall. During isovolumic relaxation, the sudden deceleration of the blood during diastole applies less torque on the impeller, causing speed to increase. Thus, when the native heart contractions are of sufficient magnitude, the speed waveform exhibits an oscillatory pattern whose fundamental frequency is near that of the patient's HR. A minority of patients, however, may exhibit insufficient contractility to accurately determine their HR, and thus the ALI calculation may have to be based purely on the SMA parameter.

Several research groups have suggested that both HR and SMA are necessary to estimate metabolic energy expenditure (35–38). Indeed, taking either of these parameters in isolation would leave such an estimate prone to both false-positive or false-negative errors. For example, spurious HRs not reflecting the demands of exercise can be caused by tachyarrhythmias, to which HF patients are prone; bradyarrhythmias, as caused by the use of beta-blocking drugs to control sympathetic overdrive; the presence of a pacemaker; and inherent chronotropic impairment apparent in certain HF patients (39–41). The SMA parameter can report false-positive errors (i.e., indicate a change in activity when none occurs) due to bodily movement unrelated to physical exertion, such as traveling in a vehicle or an elevator (26). Thus, it is proposed that a change in an individual's estimated activity level should be considered valid only when both of these variables are shifting in the same direction. Simple functions that may be used for this task are the harmonic mean or geometric mean. However, other more complex functions may be required. In any case, the ALI might then be defined as a function of SMA and HR, which results in a continuous index defined for each patient, corresponding to the full range of activity levels from rest to vigorous exercise. If it is determined that the patient's HR either cannot be reliably calculated, or exhibits no response to exercise, then the control strategy may have to be simplified to use SMA alone. Anecdotal evidence from physicians (Dr. Robert Salamonsen, The Alfred Hospital, Melbourne) observing the response of implant recipients to exercise suggests that significant HR increases are observed in most patients unless they are taking beta-blocker drugs. Thus, it is hoped that both SMA and HR variables can be applied to the majority of patients.

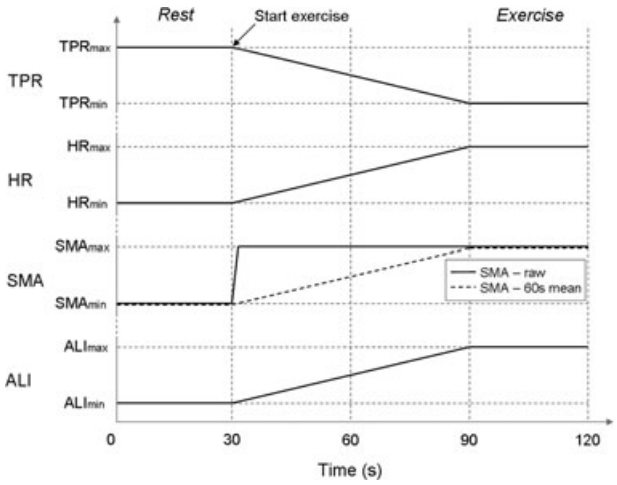

FIG. 1. Simplified representation of key parameters associated with the transition between rest and exercise states. Total peripheral resistance (TPR) and HR indicate the physiological response to exercise, while the SMA plot illustrates the wearer's physical motion. ALI is a function of HR and the SMA averaged over a 60-s interval.

The time course of changes exhibited by the various bodily compartments at the onset of exercise is quite intricate. If an individual begins strenuous exercise from a resting state, their HR will begin to rise after approximately 2 s and plateau after 30 s, their total peripheral resistance (TPR) starts to decline after 5–10 s and stabilizes after 60–90 s, and their CO rises within the first second (if there is a sufficient increase in mean circulatory pressure, otherwise sympathetic stimulation acts to increase CO after 5 s) and reaches a stable value after 40 s (34). Because the focus of the simulations performed for this study was on a comparison between rest and exercise states, as opposed to the dynamics of the transition between these states, a simplified timing scheme was used (Fig. 1). Both TPR and HR are assumed to transition from rest to exercise linearly over 60 s. Furthermore, the SMA was chosen to be

averaged over this same period, so that the SMA input to the ALI function follows a similar pattern to that associated with HR. Thus, there is a simple linear relationship between ALI, SMA, and HR:

$$HR_{normalized}(t) = \begin{cases} 0, & HR(t) < HR_{MIN} \\ \dfrac{HR(t) < HR_{MIN}}{HR_{MAX} < HR_{MIN}}, & HR_{MIN} \le HR(t) \le HR_{MAX} \\ 1, & HR_{MAX} < HR(t) \end{cases} \quad (2)$$

$$SMA_{normalized}(t) = \begin{cases} 0, & SMA(t) < SMA_{MIN} \\ \dfrac{SMA(t) < SMA_{MIN}}{SMA_{MAX} < SMA_{MIN}}, & SMA_{MIN} \le SMA(t) \le SMA_{MAX} \\ 1, & SMA_{MAX} < SMA(t) \end{cases} \quad (3)$$

$$ALI(t) = \frac{HR_{normalized}(t) + SMA_{normalized}(t)}{2} \quad (4)$$

where: $HR(t)$ = heart rate at time t.

HR_{MIN}, HR_{MAX} = resting (minimum) and active (maximum) HR as defined by implant recipient's physician.

SMA_{MIN}, SMA_{MAX} = resting (minimum) and active (maximum) SMA as defined by implant recipient's physician.

The primary role of the ALI in a demand-responsive control strategy is to determine the target value of the controlled variable, which may include one of the following:

1. Pump impeller speed (N)
2. Pump flow rate estimate (Q_{est})—based on a function of pump speed, power, and hematocrit (HCT) value (13,42)
3. Peak of pump differential pressure estimate (ΔP_{est})—pump differential pressure is estimated from Q_{est} and N (43). The peak value is taken as the control variable because this corresponds to the pressure generated during diastole, when left ventricular pressure (LVP) is at a minimum.

Due to the flatness of its characteristic differential pressure-flow curve, the Ventrassist pump has an inherent ability to increase its output flow following a drop in its observed afterload (as generally occurs during exercise) when operating at a constant target speed (44). Therefore, it would seem prudent to take advantage of this behavior and use pump speed as the basic control variable. Controlling a target ΔP would also provide similar inherent increases in flow rate; however, because it is an estimated parameter, the speed signal is thought to be more reliable as the primary control variable. The multiobjective control strategy outlined below will discuss what other variables need to be controlled in order to meet the physiological requirements.

Existing control strategies for comparison

A number of control strategies have been proposed by various research groups in the area of RBP control (7,15–18,20,22–24,45–48). Two of the most popular strategies involve control of the pulse amplitude (or pulsatility) of either a pump feedback signal (speed or current) or pump flow (either estimated or measured) and the differential pressure generated by the pump. These two strategies have been implemented in the simulation study herein, and subsequently evaluated and compared with the multiobjective control method proposed below.

Pulsatility index (PI) control

While a number of different measures of pulsatility have been investigated, in this scenario the pulsatility (i.e., maximum minus minimum over a cardiac cycle) of the speed signal—referred to as the PI—is controlled to a target level. The rationale here is that this PI is an indicator of ventricular preload, or LAP. Current theory suggests that as preload rises, so too does PI, and vice versa (4,14). As more blood is drawn from the LV with increasing pump speed (or a declining TPR, as in exercise), PI decreases until such time as excessive unloading induces a state of ventricular collapse. Thus, with the exception of near-asystolic patients who may lack sufficient native heart contractility, sustaining a target PI ensures that the pump responds to changing preload and afterload conditions by providing the highest possible flow rate short of inducing ventricular suction.

Differential pressure control

The motivation for this control principle is that the body's arterial pressure regulatory mechanism varies the vascular resistances and fluid volumes to maintain the required blood flow with an almost constant mean arterial pressure (MAP) (49). As identified by Giridharan and Skliar (19), maintaining a prescribed ΔP effectively synchronizes the assisted and natural perfusion, thus indirectly incorporating natural cardiovascular regulation into the RBP control.

An estimate of pump differential pressure (ΔP_{est}) may be calculated from the pump flow estimate and pump speed. The peak value of ΔP_{est} over a cardiac cycle (ΔP_p) is taken as the control variable because this corresponds to the pressure generated during

diastole, when LVP is at a minimum. As such, this parameter is much less affected by the native heart contractions than the minimum ΔP (i.e., that occurring during systole). The relationship between these pressures is given in Eq. 5:

$$AoP = LVP + \Delta P - P_{cannulae} \quad (5)$$

where AoP refers to aortic pressure and $P_{cannulae}$ to the pressure drop across the pump cannulae. During diastole, when LVP is near-zero (or more accurately, near-LAP) and ΔP is at its peak,

$$\Delta P_p = AoP - LVP + P_{cannulae} \approx AoP + P_{cannulae} \quad (6)$$

Considering that $P_{cannulae}$ can be estimated via an estimate of pump flow and HCT in conjunction with knowledge of the cannulae dimensions (using fluid mechanics theory), we have that the peak of ΔP provides an approximate estimate of AoP.

Multiobjective ALI-based control

A combination of the above control strategies, in which a set of goals are asserted as desirable, shall also be evaluated. Specifically, a hierarchical set of objectives shall be imposed, in decreasing priority:

1 Pump power must remain below a certain threshold.
2 A minimum pump flow must always be achieved.
3 Upon detection of ventricular suction, pump speed must be reduced.
4 A minimum PI must always be achieved.
5 Peak ΔP must remain within a specified range.
6 Speed to be controlled according to ALI.

It is hypothesized that by using the above set of constraints, the physiological requirements set out earlier will be satisfied. Imposing a minimum pump flow will ensure the provision of a minimum CO. The alleviation and avoidance of suction via the minimum PI and suction detection modules guarantees LAP remains in a safe range. The provision of a peak ΔP range limits the range of arterial pressure generated and the ALI-based speed controller will provide a CO increase during exercise, unless otherwise constrained. The integrity of the pump hardware is maintained by the maximum pump power requirement. As mentioned earlier, the algorithms dealing with the estimation of pump flow and differential pressure, as well as the detection of suction, have been developed by the authors' research group in recent years (6,8,10–13) and now form the foundation of the present control strategy. Figure 2 illustrates this strategy in terms of a flow chart.

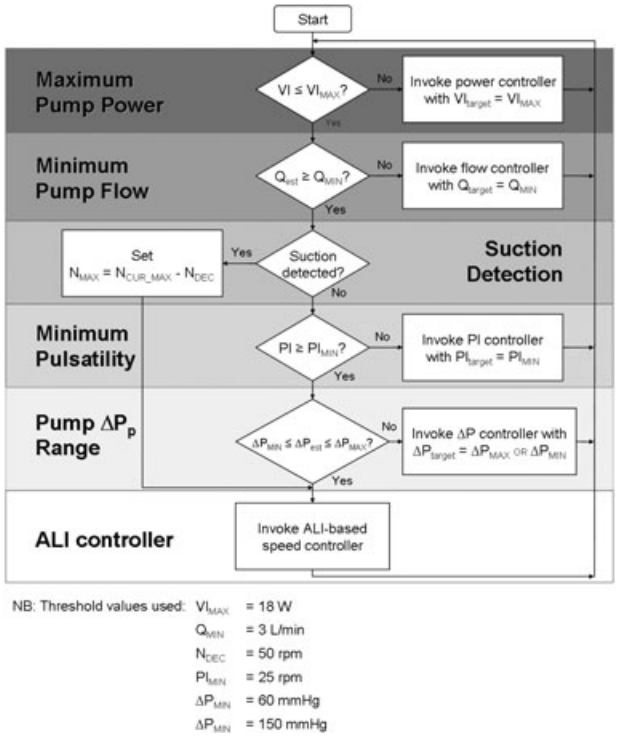

FIG. 2. Flowchart of multiobjective control strategy. Nomenclature: VI = pump power (maximum over control period, T_{ctrl}), VI_{MAX} = maximum power threshold, Q_{est} = average pump flow estimate (average over T_{ctrl}), Q_{MIN} = minimum flow threshold, Q_{target} = target flow value, N_{CUR_MAX} = current maximum speed threshold, N_{MAX} = maximum speed threshold, N_{DEC} = speed decrement upon suction detection, PI = pulsatility index (average over T_{ctrl}, excluding speed changes), PI_{MIN} = minimum PI threshold, PI_{target} = target PI value, ΔP_{est} = current peak ΔP estimate (maximum over T_{ctrl}), ΔP_{MAX} = maximum peak ΔP threshold, ΔP_{MIN} = minimum peak ΔP threshold, ΔP_{target} = target peak ΔP value.

Software model

In order to evaluate the proposed control strategy, a software model incorporating a lumped-parameter model of the CVS in combination with a model of the RBP under examination was used. As reported previously (50), the CVS model comprises 12 compartments including the left and right sides of the heart and the pulmonary and systemic circulations, and allows the setting of ventricular interaction via the interventricular septum and pericardium. Three differential equations are used to model the hydraulic and electrical characteristics of the pump:

1 Motor windings electrical equation

$$V = k_e \omega_e + RI + L\frac{dI}{dt}, \quad (7)$$

where V is motor terminal voltage (V), $k_e = 8.48e-3$ V/rad/s is the BEMF constant, ω_e is the elec-

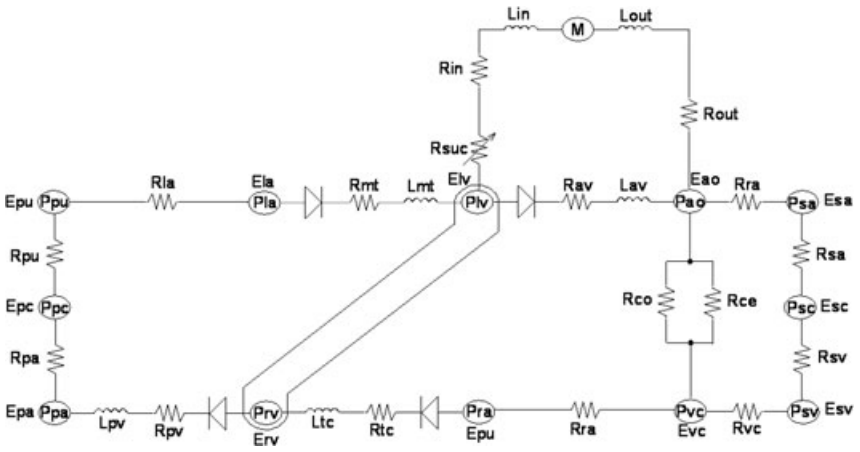

FIG. 3. Electrical equivalent circuit analog of the human cardiovascular system model combined with the lumped parameter model of the pump and cannulae. For clarity, the capacitive elements (Ci = 1/Ei) representing the compliance of the various compartments are not shown, nor are the resistive elements representing the viscoelastic properties of the pulmonary artery and the aorta (sourced from [50]).

trical speed ($\omega_e = 2\omega$, where ω is the impeller speed in rad/s), I is the motor phase current (A), $R = 1.38\ \Omega$ is the motor winding resistance, and $L = 0.439$ mH is the motor winding inductance.

2 Electromagnetic torque transfer equation

$$T_e = 3k_e I = J\frac{d\omega}{dt} + f(Q,\omega)$$
$$f(Q,\omega) = aQ^2\omega + bQ\omega^2 + c\omega + d\omega^3 \quad (8)$$

where T_e is the input electromagnetic torque (kg/m^2/s^2), Q is the pump flow rate (L/min), and J = 7.74e – 6 kg/m^2 is the moment of inertia of the impeller. Polynomial coefficients were obtained by least squares fitting of the experimental data obtained under steady flow conditions (50).

3 Pump hydraulic equation (50).

$$\Delta P = e + fQ^3 + g\omega^2 \quad (9)$$

where ΔP is the differential pressure across the pump (mm Hg), $e = -6$ mm Hg, $f = -0.0524$ mm Hg/L^3/min^3, and $g = 0.0019$ mm Hg/rpm^3.

In addition, the inflow and outflow cannulae are each modeled in terms of a constant flow resistance (R_{in} and R_{out} in Fig. 3) which causes a pressure drop, and a series inductance (L_{in} and L_{out}) which resists changes in flow rate. A third resistance (R_{suc}) is included prior to the inflow cannula to simulate suction events. The magnitude of this variable resistance is a function of LVP (51). An electrical equivalent circuit analog of the combined model is illustrated in Fig. 3.

Software simulation protocol

Initial software simulations were performed with the LVAD removed from the model in order to demonstrate the validity of the CVS model alone. The model was first tested with cardiovascular parameters associated with normal healthy adults, followed by a simulation of three class IV (NYHA functional classification) HF cases of varying severity (Table 1). The software model parameters associated with each case were carefully chosen in order to ensure the most realistic simulation—in terms of CO, aortic pressure, LAP, and TPR—was achieved. Data from

TABLE 1. *Software model parameter values used in normal and heart failure modes, both at rest and during exercise*

	Normal		Heart failure					
			Rest			Exercise		
Model parameter	Rest	Exercise	1	2	3	1	2	3
E_{max} LV (mm Hg/mL)	4.7	9.4	1.5	1	0.5	2.25	1.5	0.75
E_{max} RV (mm Hg/mL)	0.54	1.08	0.28	0.21	0.14	0.35	0.26	0.18
HR (bpm)	70	150	80	85	90	135	120	110
Aortic resistance (mm Hg/mL/s)	0.48	0.16	0.72	0.36	0.72	0.36	0.72	0.36
Systemic arterial resistance (mm Hg/mL/s)	0.5	0.17	0.5	0.25	0.5	0.25	0.5	0.25
Systemic venous resistance (mm Hg/mL/s)	0.22	0.07	0.22	0.11	0.22	0.11	0.22	0.11
Vena cava resistance (mm Hg/mL/s)	0.08	0.03	0.08	0.04	0.08	0.04	0.08	0.04

HR, heart rate; LV, left ventricle; RV, right ventricle.

Epstein et al. (52) were used to validate these input parameters.

Subsequent simulations of the HF cases were performed with the LVAD model included, and these were used to evaluate the proposed and existing control strategies. Each simulation commenced in a state of physical inactivity (rest), followed by a single transition from rest to an active state (exercise), whereby each of the variables of interest undergo a linear change between the specified threshold values (Table 2). For the constant speed, PI, and peak ΔP control modes, the target values are fixed across rest and exercise, as described earlier.

In total, four separate strategies were simulated: constant speed, PI, peak differential pressure, and multiobjective ALI-based control. To ensure an accurate comparison between these strategies could be made, the target control variables assigned for each method were carefully selected (Table 2). The target speed value for the constant speed control mode was selected in the same manner as prescribed clinically for the Ventrassist LVAD—that is, the speed at which the PI is 90% of its maximum value. Constant speed control represents the current strategy used in the field and formed the basis for comparison with the automatic control modes. The target values for PI, peak ΔP, and resting speed in ALI-based control were chosen to coincide with the corresponding values obtained in the rest phase of the constant speed control simulation. During the exercise phase, the PI and peak ΔP target values remain the same, while for the ALI-based control mode, the target speed is set to the speed at which suction occurs (at rest) (see Table 2). In clinical practice, this speed would be set lower; however, here we wish to examine the ability of this control method to avoid suction without prior knowledge of the speed at which it is likely to occur.

TABLE 2. *Target values used for each of the control modes in both the rest and exercise states*

		Activity state	
Control mode	HF case	Rest	Exercise
Constant speed (rpm)	1	2020	
	2	2000	
	3	1880	
Pulsatility index (rpm)	1	135	
	2	87	
	3	40	
Peak ΔP (mm Hg)	1	91.2	
	2	84.4	
	3	70.3	
Activity level index (Speed targets) (rpm)	1	2020	2620
	2	2000	2520
	3	1880	2350

For the constant speed, PI and peak ΔP control modes, the target values are fixed across rest and exercise.

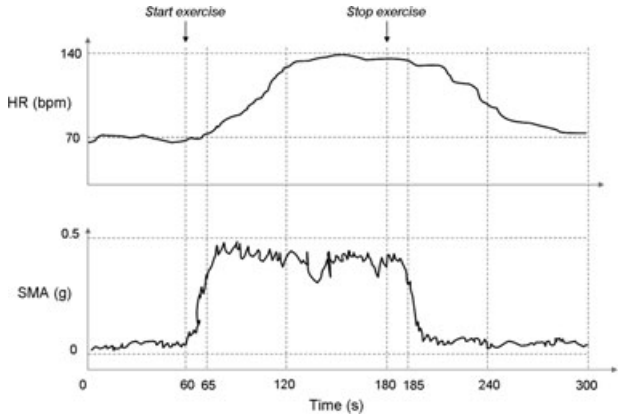

FIG. 4. A recording of SMA and HR data collected from a healthy person undergoing transitions between rest and exercise (using a treadmill), with exercise commencing at 60 s and ceasing at 180 s.

Due to the nature of these simulations, the ALI will necessarily be a simulated value. As such it will transition in a linear fashion from its minimum to its maximum value. An example of real data from a healthy individual undertaking an exercise task is provided to aid the reader's understanding of the signals involved (Fig. 4).

RESULTS

The primary performance measure used to distinguish between the various control strategies tested is the increase in pump flow from rest to exercise, while the avoidance of ventricular suction and regurgitant pump flow were also significant. As described earlier, the resting pump operating point for all control modes was chosen to coincide with the baseline target speed selected for constant speed control. Thus, the pump flow values in the resting state are constant across all test simulations (Table 3), with the exception of the ALI-based control mode for case 3, where the minimum flow constraint of 3 L/min was imposed. Table 3 indicates the absolute and relative flow increase between rest and exercise for each control mode, as well as comparing this flow increase with that attained during the constant speed control mode.

The pump flow increases attained with a constant target speed—1.95, 1.63, and 1.36 L/min for HF cases 1, 2, and 3, respectively—serve as a benchmark upon which other flow changes shall be assessed (Fig. 5a).

With regard to the ALI-based control mode, pump flow increases of 2.54, 1.94, and 1.15 L/min were achieved for the three HF cases, from rest to exercise. Compared with constant speed control, this represents a relative flow increase of 30.3, 19.8, and

TABLE 3. *Statistical summary of software simulation results*

Control mode	HF case	Pump flow		Pump flow increase		Pump flow increase relative to constant speed mode		Average pump speed		Pulsatility index
		Rest	Exercise	Absolute	Relative	Absolute	Relative	Rest	Exercise	Exercise
		L/min	L/min	L/min	%	L/min	%	rpm	rpm	rpm
Constant speed	1	3.58	5.53	1.95	54.5	—	—	2020	2020	118
	2	3.28	4.90	1.63	49.4	—	—	2000	2000	72
	3	2.67	4.03	1.36	50.9	—	—	1880	1880	39
Pulsatility index	1	3.58	3.92*	0.34*	9.5*	–1.61*	–82.6*	2022	1800	102
	2	3.28	4.80	1.52	46.3	–0.10	–6.2	1998	1929	87.5
	3	2.65	4.01	1.36	51.3	0.00	0.0	1875	1872	40
Peak ΔP	1	3.58	6.14	2.56	71.5	0.61	31.3	2021	2400	22
	2	3.28	5.52	2.24	68.3	0.62	38.3	2003	2311	4
	3	2.68	4.44	1.76	65.7	0.40	29.4	1884	2084	4
Activity level index	1	3.58	6.12	2.54	71.0	0.59	30.3	2020	2387	25
	2	3.28	5.22	1.94	59.2	0.32	19.8	2000	2194	25
	3	3.00	4.15	1.15	38.3	–0.21	–15.4	2050	1955	25

Note: Changes in pump flow between rest and exercise states occurring for each control mode, and comparisons with the baseline values encountered in constant speed control are presented. The PI is given as an indication of the proximity to ventricular suction in the exercise state.

* For HF case 1 in the PI control mode, the aortic valve was opening during exercise. The mean flow through the aortic valve in this case was 1.52 L/min, providing a cardiac output of 5.44 L/min.

–15.4%, respectively. In the third and most severe HF case (Fig. 5b), the minimum flow constraint was imposed to bring the resting flow rate up to 3 L/min; the pump speed required to provide this flow rate was 2050 rpm, whereas the original target speed was 1880 rpm. In addition, the speed amplitude control module was activated to ensure a minimum PI was maintained and suction was avoided, resulting in a pump speed of 1955 rpm. The combination of these two constraints being satisfied meant the flow increase was greater for the constant speed control case.

Simulations of the reverse transitions—that is, from exercise to rest—were also performed and resulted in essentially a mirror image of the plots in Fig. 5.

In general, the smallest increases in pump flow were observed with PI control. Because the model produces a fall in PI from rest to exercise at a constant target speed, it follows that average pump speed must be reduced in a PI controller so that the target PI value is maintained. Thus, the pump flow increases were actually of smaller magnitude than those observed in constant speed control mode. For HF case 1, the PI target value of 135 rpm could not be reached, and so the minimum pump speed threshold of 1800 rpm was imposed. At this low speed, the aortic valve opened during systole, thus allowing aortic valve flow to contribute in addition to pump flow toward CO.

Peak ΔP control provided the largest increases in pump flow, and highest flows overall (Fig. 5c). The relative pump flow increases compared with constant speed control are 31.3, 38.3, and 29.4% for HF cases 1, 2, and 3, respectively (Table 3). It should be noted, however, that the PI values in exercise were 22, 4, and 4 rpm, respectively. These values are all below the nominated minimum PI threshold of 25 rpm, and thus represent a potentially dangerous state for the patient. Furthermore, the resting pump flow in HF case 3 is 2.68 L/min which, although similar to that obtained for constant speed control, is significantly below the minimum flow threshold for adequate perfusion.

DISCUSSION

A number of control strategies have been proposed by research groups in the RBP field. Particular control elements were identified as having the ability to satisfy certain physiological requirements and were adapted for inclusion in the ALI-based strategy presented.

The University of Pittsburgh team headed by Antaki have reported the implementation of various control indices, including those based on flow pulsa-

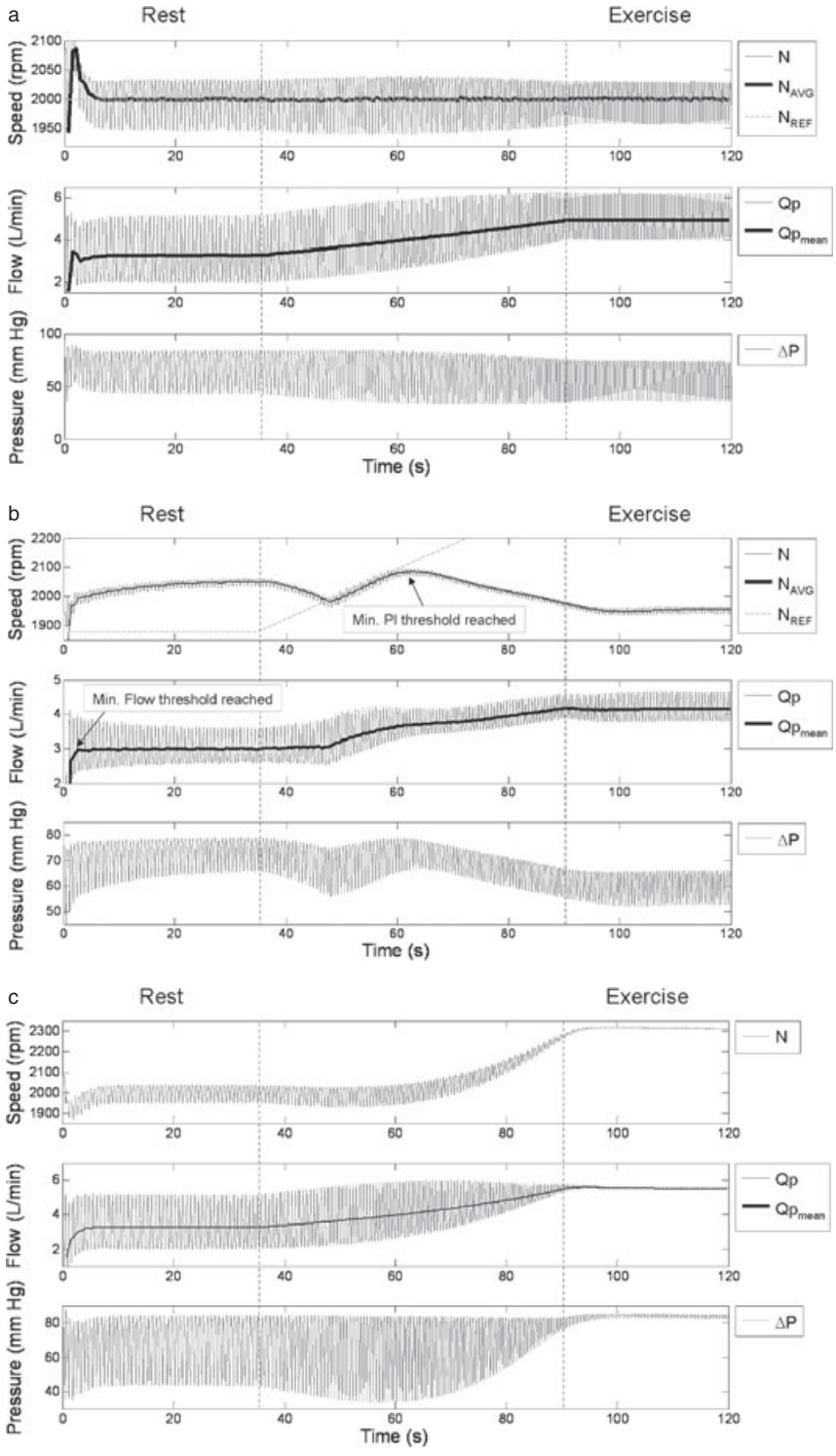

FIG. 5. Results of the software simulations for (a) constant speed control (HF case 2), (b) HF case 3 of ALI-based control, and (c) ΔP control (HF case 3). The left and right vertical dashed lines indicate the start of exercise and end of transition to exercise, respectively.

tility (4), pulsatility ratio (defined as flow pulsatility divided by head pulsatility) (14,15), and strategies using a combination of indices to satisfy several constraints (24,45,53,54). Studies by Fu and Xu (17) and Endo et al. (16) also support the efficacy of pulsatility indices (namely, flow pulsatility and normalized motor current amplitude, respectively) as control parameters. The present study utilized the pulsatility in pump speed primarily as an indicator of suction proximity.

Giridharan et al. (18–21) proposed that maintaining an average reference ΔP was an appropriate strategy for LVAD control, as it indirectly incorporated natural cardiovascular regulation by maintaining a stable MAP. Wu et al. (23) used an optimal controller to minimize the sum of the aortic pressure tracking error and weighted differential pressure tracking error, in an attempt to not only maintain a desired aortic pressure, but to avoid the occurrence of ventricular collapse. The authors of the present study have chosen to use the pump ΔP (specifically the peak of ΔP over a cardiac cycle) as a parameter that can assist in maintaining the patient's arterial pressure within safe bounds.

Ohuchi et al. (55) proposed a control strategy in which a target pump speed was set according to the measured HR, by relating HR with CO, and pump flow with pump speed. HR was determined via electrocardiogram (as opposed to a noninvasive estimate) recording with external electrodes—an undesirable approach for long-term use by the implant recipients. Schima et al. (47) and Vollkron et al. (48) have reported on the successful implementation of an HR-based control strategy in clinical studies. At the heart of the technique is a desired flow rate setting based on HR, while the operating point is also determined by pump power and pump flow pulsatility. The automatic control strategy presented in Schima et al. (47) provided a pump flow increase of 0.94 ± 0.50 L/min ($P < 0.05$) and an associated increase in work capacity of 8% (mean for five subjects), in response to physical activity. As evidenced by these studies, incorporating indicators of patient activity into a control method is considered essential for attaining the highest possible increase in their exercise capacity. The ALI-based strategy uses HR as one of two inputs to determine the patient's ALI, which is in turn related to a target pump speed setting.

Previous discussions of pulsatility-related indices have generally agreed that while the amplitude of pulsatility in the pump feedback signals is a useful indicator of the imminence of ventricular suction, it cannot be used as a single index for control purposes. As pointed out in Choi et al. (15), pulsatility-based control necessarily requires a suction detection mechanism in operation to distinguish between pulsatility in the normal pumping state from that encountered during the suction state. Assuming a suction alleviation mechanism is active, a strategy which involves the tracking of a target pulsatility level—to provide a maximal flow without inducing suction—fails to consider any negative impact on arterial pressure (45). Furthermore, clinical evidence suggests that pulsatility decreases during exercise due to increased flow (47); therefore, a PI controller whose target value remains static would act to decrease pump speed during exercise. It would seem sensible to increase speed as much as possible during exercise, provided a minimum PI threshold was met to avoid the occurrence of suction. Indeed, a strategy with a variable target PI—such that the resting PI was higher than that prescribed during exercise—based on the patient's activity level would provide a similar result to the ALI-based strategy presented herein. Perhaps the point here is that the target PI need not be a small value (such as the minimum PI threshold) during rest, as this may produce a high arterial pressure or more blood flow than the patient requires during rest, as well as increasing the risk of ventricular suction due to sudden drops in preload (e.g., during postural transitions).

Perhaps the leading advocate of ΔP control is Giridharan (18–21). The idea of attempting to maintain a steady MAP within acceptable bounds is indeed valid, as evidenced by the group's results and discussion. Once again though, we also must consider the other critical physiological requirements. Controlling an estimate of pump ΔP or MAP with no other constraints may lead to ventricular suction or an undesirable CO value under certain circumstances.

Given the above limitations with using a single control index in isolation, it is apparent that a combination of objectives must be asserted as desirable in order to satisfy multiple physiological requirements.

The ALI-based control technique presented herein was successful in achieving the stated objectives in a software simulation environment. Pump flow increases in excess of those obtained by the inherent increases of constant speed control were recorded for two of the three HF cases. In the most severe HF case, the constraints of minimum pump flow and speed pulsatility were effectively imposed to restore a minimum prescribed flow and ensure suction was well avoided. Despite the relatively lower flow increase in this case, the resulting operating point posed no safety risk to the simulated patient. It is clear in such cases that the patient's physical activity limit has been reached, with right heart output unable to increase its supply to the LV.

As stated in the results section, PI control resulted in relatively lower flows during exercise, confirming the inadequacy of such a control technique unless a variable activity-based PI target with restrictions on peak ΔP is adopted, as discussed above. Despite the relatively higher flows achieved by peak ΔP control in all HF cases during exercise, the proximity of the LV to suction represented a potentially dangerous state

for the patient. Furthermore, the resting pump flow in HF case 3 is significantly below the minimum flow threshold for adequate perfusion. Thus, the results demonstrate that if all physiological requirements are considered, the ALI-based hierarchical control method leads to a superior outcome for the implant recipient.

As indicated by the values in Table 1, the transition from rest to exercise involved the change of variables associated with ventricular contractility, HR, and the resistance of several peripheral compartments. One of the key parameters that we can derive from these changes is the TPR. TPR varied from 1.38–1.45 mm Hg/mL/s during the rest phase, and 0.75–0.82 mm Hg/mL/s during the exercise phase, across all simulations. This compared favorably with data from Epstein et al. (52) which reports a mean TPR of 1.53 ± 0.33 mm Hg/mL/s at rest and 0.72 ± 0.27 mm Hg/mL/s during maximal exercise, for 21 patients with various types of heart disease.

Due to the wide variation in both HR and SMA values representative of physical activity (26,28,52), each implant recipient would need to undertake a calibration test in a postoperative clinical scenario, and perhaps subsequent routine tests to account for any improvement or deterioration in their condition. Such a calibration test may determine the resting and maximal exercise HR and SMA threshold values via the following procedure:

- Resting HR and SMA should be acquired when the patient is supine for at least 5 min, ensuring the absence of arrhythmia.
- Maximal exercise HR and SMA should be obtained following a treadmill test whereby the patient ambulates at a steadily increasing speed until they are fatigued and wish to stop. The last recording of HR and SMA would then define the respective threshold values for exercise.

Once the HR and SMA thresholds are ascertained, the ALI function may be incorporated into the control strategy.

Having attained satisfactory results and experience in the software environment, the next step in the research will be to test the ALI-based strategy in an animal model, followed by clinical studies. In addition to these studies, there are also a number of other research paths requiring investigation. At present, the multiobjective strategy is based solely upon an estimate of the patient's level of physical activity. There are other factors, however, that may influence their hemodynamic state. Changes in posture, or performing the Valsalva maneuver, may result in relatively rapid changes in cardiac filling, and venous or arterial pressures. While it is envisaged that the minimum PI and pump flow requirements of the control strategy would assist in these scenarios, they have not been simulated and remain a task for future studies.

CONCLUSION

A noninvasive control strategy for an RBP based on an estimate of the implant recipient's physical activity level has been presented. With provisions for the avoidance and alleviation of ventricular suction, and boundaries asserted for estimates of pump flow and differential pressure, the control strategy was successful in satisfying key physiological requirements when simulated in a software environment. The results demonstrated a platform from which further investigations can proceed.

REFERENCES

1. Australian Institute of Health and Welfare. *Australia's Health 2004*. Canberra: Australian Federal Government, 2004.
2. Ni H. Prevalence of self-reported heart failure among US adults: results from the 1999 National Health Interview survey. *Am Heart J* 2003;146:121–8.
3. British Heart Foundation Health Promotion Research Group. Coronary heart disease statistics. *British Heart Foundation Statistics Website*. 2008.
4. Choi S, Antaki JE, Boston R, Thomas D. A sensorless approach to control of a turbodynamic left ventricular assist system. *IEEE Trans Control Syst Technol* 2001;9:473–82.
5. Amin DV, Antaki JF, Litwak P, et al. Controller for an axial-flow blood pump. *Biomed Instrum Technol* 1997;31:483–7.
6. Karantonis DM, Lovell NH, Ayre PJ, Mason DG, Cloherty SL. Identification and classification of physiologically significant pumping states in an implantable rotary blood pump. *Artif Organs* 2006;30:671–9.
7. Yuhki A, Hatoh E, Nogawa M, Miura M, Shimazaki Y, Takatani S. Detection of suction and regurgitation of the implantable centrifugal pump based on the motor current waveform analysis and its application to optimization of pump flow. *Artif Organs* 1999;23:532–7.
8. Ayre PJ, Vidakovic SS, Tansley GD, Watterson PA, Lovell NH. Sensorless flow and head estimation in the VentrAssist rotary blood pump. *Artif Organs* 2000;24:585–8.
9. Wakisaka Y, Okuzono Y, Taenaka Y, et al. Noninvasive pump flow estimation of a centrifugal blood pump. *Artif Organs* 1997;21:651–4.
10. Ayre PJ, Lovell NH. Identifying physiologically significant pumping states in implantable rotary blood pumps using non-invasive system observers. *25th Annual International Conference of the IEEE Engineering in Medicine and Biology Society*. Cancun, Mexico. IEEE 2003;1:439–42.
11. Ayre PJ, Lovell NH, Woodard JC. Non-invasive flow estimation in an implantable rotary blood pump: a study considering non-pulsatile and pulsatile flows. *Physiol Meas* 2003;24:179–89.
12. Karantonis DM, Mason DG, Salamonsen RF, Ayre PJ, Cloherty SL, Lovell NH. Classification of physiologically significant pumping states in an implantable rotary blood pump: patient trial results. *ASAIO J* 2007;53:617–22.
13. Malagutti N, Karantonis DM, Cloherty SL, et al. Noninvasive average flow estimation for an implantable rotary blood pump: a new algorithm incorporating the role of blood viscosity. *Artif Organs* 2007;31:45–52.

14. Choi S, Boston J. An investigation of the pump operating characteristics as a novel control index for LVAD control. *Int J Control Autom* 2005;3:100–8.
15. Choi S, Boston JR, Antaki JF. Hemodynamic controller for left ventricular assist device based on pulsatility ratio. *Artif Organs* 2007;31:114–25.
16. Endo G, Araki K, Kojima K, Nakamura K, Matsuzaki Y, Onitsuka T. The index of motor current amplitude has feasibility in control for continuous flow pumps and evaluation of left ventricular function. *Artif Organs* 2001;25:697–702.
17. Fu M, Xu L. Computer simulation of sensorless fuzzy control of a rotary blood pump to assure normal physiology. *ASAIO J* 2000;46:273–8.
18. Giridharan GA, Skliar M. Nonlinear controller for ventricular assist devices. *Artif Organs* 2002;26:980–4.
19. Giridharan GA, Skliar M. Control strategy for maintaining physiological perfusion with rotary blood pumps. *Artif Organs* 2003;27:639–48.
20. Giridharan GA, Skliar M. Physiological control of blood pumps using intrinsic pump parameters: a computer simulation study. *Artif Organs* 2006;30:301–7.
21. Giridharan GA, Skliar M, Olsen DB, Pantalos GM. Modeling and control of a brushless DC axial flow ventricular assist device. *ASAIO J* 2002;48:272–89.
22. Waters T, Allaire P, Tao G, et al. Motor feedback physiological control for a continuous flow ventricular assist device. *Artif Organs* 1999;23:480–6.
23. Wu Y, Allaire P, Tao G, Wood H, Olsen D, Tribble C. An advanced physiological controller design for a left ventricular assist device to prevent left ventricular collapse. *Artif Organs* 2003;27:926–30.
24. Boston JR, Simaan MA, Antaki JF, Yih-Choung Y, Seongjin C. Intelligent control design for heart assist devices. *Proceedings of the 1998 IEEE International Symposium on Intelligent Control (ISIC)*. Gaithersburg, MD. IEEE 1998;497–502.
25. Hendelman D, Miller K, Baggett C, Debold E, Freedson P. Validity of accelerometry for the assessment of moderate intensity physical activity in the field. *Med Sci Sports Exerc* 2000;32:S442–9.
26. Bouten CV, Koekkoek KT, Verduin M, Kodde R, Janssen JD. A triaxial accelerometer and portable data processing unit for the assessment of daily physical activity. *IEEE Trans Biomed Eng* 1997;44:136–47.
27. Bouten CV, Verboeket-van de Venne WP, Westerterp KR, Verduin M, Janssen JD. Daily physical activity assessment: comparison between movement registration and doubly labeled water. *J Appl Physiol* 1996;81:1019–26.
28. Mathie MJ, Coster AC, Lovell NH, Celler BG, Lord SR, Tiedemann A. A pilot study of long-term monitoring of human movements in the home using accelerometry. *J Telemed Telecare* 2004;10:144–51.
29. Mathie MJ, Coster AC, Lovell NH, Celler BG. Accelerometry: providing an integrated, practical method for long-term, ambulatory monitoring of human movement. *Physiol Meas* 2004;25:R1–20.
30. Mathie MJ, Lovell NH, Coster ACF, Celler BG. Determining activity using a triaxial accelerometer. *Proceedings of the Second Joint EMBS/BMES Conference [Engineering in Medicine and Biology, 2002. 24th Annual Conference and the Annual Fall Meeting of the Biomedical Engineering Society]*. Houston, TX. IEEE 2002;3:2481–2.
31. Dauncey MJ, James WP. Assessment of the heart-rate method for determining energy expenditure in man, using a whole-body calorimeter. *Br J Nutr* 1979;42:1–13.
32. Payne PR, Wheeler EF, Salvosa CB. Prediction of daily energy expenditure from average pulse rate. *Am J Clin Nutr* 1971;24:1164–70.
33. Rennie KL, Hennings SJ, Mitchell J, Wareham NJ. Estimating energy expenditure by heart-rate monitoring without individual calibration. *Med Sci Sports Exerc* 2001;33:939–45.
34. Guyton AC, Jones CE, Coleman TG. *Cardiac Output and Its Regulation*. Philadelphia, PA: Saunders, 1973.
35. Eston RG, Rowlands AV, Ingledew DK. Validity of heart rate, pedometry, and accelerometry for predicting the energy cost of children's activities. *J Appl Physiol* 1998;84:362–71.
36. Moon JK, Butte NF. Combined heart rate and activity improve estimates of oxygen consumption and carbon dioxide production rates. *J Appl Physiol* 1996;81:1754–61.
37. Strath SJ, Brage S, Ekelund U. Integration of physiological and accelerometer data to improve physical activity assessment. *Med Sci Sports Exerc* 2005;37:S563–71.
38. Treuth MS, Adolph AL, Butte NF. Energy expenditure in children predicted from heart rate and activity calibrated against respiration calorimetry. *Am J Physiol* 1998;275:E12–8.
39. Borlaug BA, Melenovsky V, Russell SD, et al. Impaired chronotropic and vasodilator reserves limit exercise capacity in patients with heart failure and a preserved ejection fraction. *Circulation* 2006;114:2138–47.
40. Clark AL, Coats AJ. Chronotropic incompetence in chronic heart failure. *Int J Cardiol* 1995;49:225–31.
41. Colucci WS, Ribeiro JP, Rocco MB, et al. Impaired chronotropic response to exercise in patients with congestive heart failure. Role of postsynaptic beta-adrenergic desensitization. *Circulation* 1989;80:314–23.
42. Karantonis DM, Cloherty SL, Mason DG, Ayre PJ, Lovell NH. Noninvasive pulsatile flow estimation for an implantable rotary blood pump. *29th Annual International Conference of the IEEE Engineering in Medicine and Biology Society*. Lyon, France, 2007.
43. Lim E, Karantonis DM, Reizes JA, Cloherty SL, Mason DG, Lovell NH. Noninvasive average flow and differential pressure estimation for an implantable rotary blood pump using dimensional analysis. *IEEE Trans Biomed Eng* 2008;55:2094–101.
44. Tansley G, Vidakovic S, Reizes J. Fluid dynamic characteristics of the VentrAssist rotary blood pump. *Artif Organs* 2000;24:483–7.
45. Antaki JF, Boston JR, Simaan MA. Control of heart assist devices. *42nd IEEE Conference on Decision and Control*. Hawaii. IEEE 2003;4:4084–9.
46. Baloa LA, Liu D, Boston JR, Simaan MA, Antaki JF. Control of rotary heart assist devices. *American Control Conference*. Chicago, IL. IEEE 2000.
47. Schima H, Vollkron M, Jantsch U, et al. First clinical experience with an automatic control system for rotary blood pumps during ergometry and right-heart catheterization. *J Heart Lung Transplant* 2006;25:167–73.
48. Vollkron M, Schima H, Huber L, Benkowski R, Morello G, Wieselthaler G. Development of a reliable automatic speed control system for rotary blood pumps. *J Heart Lung Transplant* 2005;24:1878–85.
49. Guyton AC. *Textbook of Medical Physiology*. Philadelphia, PA: Saunders, 1986.
50. Lim E, Cloherty SL, Reizes JA, et al. A dynamic lumped parameter model of the left ventricular assisted circulation. *29th Annual International Conference of the IEEE Engineering in Medicine and Biology Society*. Lyon, France, 2007;3990–3.
51. Schima H, Honigschnabel J, Trubel W, Thoma H. Computer simulation of the circulatory system during support with a rotary blood pump. *ASAIO Trans* 1990;36:M252–4.
52. Epstein SE, Beiser GD, Stampfer M, Robinson BF, Braunwald E. Characterization of the circulatory response to maximal upright exercise in normal subjects and patients with heart disease. *Circulation* 1967;35:1049–62.
53. Boston JR, Antaki JF, Simaan MA. Hierarchical control of heart-assist devices. *IEEE Robot Autom Mag* 2003;10:54–64.
54. Boston JR, Baloa LA, Liu D, Simaan MA, Choi S, Antaki JF. Combination of data approaches to heuristic control and fault detection. *Conference on Control Applications*. Anchorage, AK, 2000;98–103.
55. Ohuchi K, Kikugawa D, Takahashi K, et al. Control strategy for rotary blood pumps. *Artif Organs* 2001;25:366–70.